2.3 Investigation on Ignition Coil Specification for Dilution Combustion System

Kazuhiro Oryoji, Kengo Kumano, Shogo Namba, Yoshihiko Akagi, Yoshifumi Uchise, Tatsuya Kuboyama, Yasuo Moriyoshi

Abstract

To improve thermal efficiency of internal combustion engine, dilution combustion system, such as lean burn and Exhaust Gas Recirculation (EGR) system, have been developed with spark ignition coils generating large discharge current and energy. Several researches have clarified that large discharge current increases discharge channel stretch and decreases possibility of discharge channel blow-off and misfire. However, these investigations don't mention effect of discharge current profile on combustion speed and discharge channel behaviour enough. Purpose of this research is to investigate relation among dilution rate, combustion speed, discharge channel behaviour and discharge current. To achieve this purpose, five coils having different current profiles were evaluated by combustion test and in-cylinder optical measurement test with research single cylinder engine. The combustion test results showed a correlation between dilution limit and initial combustion period. And optical measurement test results showed a correlation of initial combustion period with discharge channel stretch. Moreover, saturation of discharge channel stretch were observed from a certain discharge current value on up. Based on these results, adequate coil for dilution system was selected. Finally, the coil was equipped on a vehicle and performance test was conducted. The vehicle with LP-EGR system was stably driven with 18% of EGR rate, and 2.3% of fuel reduction rate were verified in the WLTC mode. The selected high energy ignition coil was contributing reduction of misfire during EGR operation.

1 Introduction

In order to prevent from global warming, regulations of CO2 emission of automotive are going to be stricter. In order to comply with future CO2 regulation, dilution combustion systems, such as lean burn and EGR (Exhaust Gas Recirculation) system, for reducing pumping loss and cooling loss, have been developed. Since air-fuel mixtures are diluted by air or EGR gas under dilution combustion condition, ignition of mixture gas by spark ignition is harder than conventional stoichiometric condition. Though conventional stoichiometric mixture is successfully ignited by tens mJ of ignition coil secondary energy, hundreds mJ of its secondary energy might be required for dilution combustion. Therefore, to clarify required coil specifications, several studies have been investigating relation between flame kernel formation and coil specifications, such as secondary current or relation between dilution limit stretch and coil specifications[1].

Shiraishi et al investigated relation between discharge channel stretch and flow velocity around spark plug or discharge current, or relation between EGR combustion limit and discharge current, and they disclosed that large discharge current increases EGR rate limit. Brandtor et al proposed ignition coil which is able to keep discharge current value at certain range for a while, and they disclosed that air-fuel ratio of stable combustion condition is increased by long duration of discharge current keep [2]. Suzuki et al clarified that flame kernel formation is prevented by shortage of energy supply due to discharge blow-off under high velocity condition and by slow laminar flame speed at discharge blow-off area[3]. These investigations, however, mentioned relation between coil specification and discharge channel behavior and relation between coil specification and EGR rate limit or air-fuel ratio limit, these have not mentioned relation between coil specification and combustion status or discharge channel behavior of each combustion cycle. With accepting this background, the purpose of this investigation is to clarify combustion status index having correlation with dilution limit of stable combustion and relation between the index and coil specification or discharge channel stretch. To achieve this purpose, five kinds of ignition coils are evaluated with optical single cylinder engine and relation among combustion status, discharge channel stretch and discharge energy were investigated. Finally, selected ignition coil was equipped on a demo vehicle and the performance was evaluated.

2 Experimental setup

In this study, combustion performance test and in-cylinder optical measurement test were conducted by using a single cylinder engine. Fig. 1 shows schematic of the single cylinder engine and table 1 shows single cylinder engine specifications. The engine works as a single cylinder engine by occurring combustion in one cylinder only. Combustion chamber type is pent roof and compression ratio is 12.2.Furthermore, a tumble adapter was equipped at intake port to increase turbulent energy as shown on left figure of fig.2.The right figure of fig.2 shows estimated value of turbulent energy by three dimensional fluid dynamics As shown on fig.2, in-cylinder turbulent energy is expected to achieve five times larger value than normal setting. To suppress variation of in-cylinder mixture distribution, fuel is supplied by port injection. Fuel is supplied by 0.26g/s and air flow rate is adjusted to achieve target air-fuel ratio. Air-fuel ratio was calculated by Brettschneider/Spridndt method [4] based on density of emission species such as HC, CO2, CO O2 and NOx measured by emission analyzer (MEXA-7100Fx). RON99.8 fuel is applied. The H/C ratio of fuel is 1.708 and stoichiometric air-fuel ratio is 14.37. Spark plug has 0.9mm gap between center electrode and ground electrode and the internal resistance is 5kΩ.

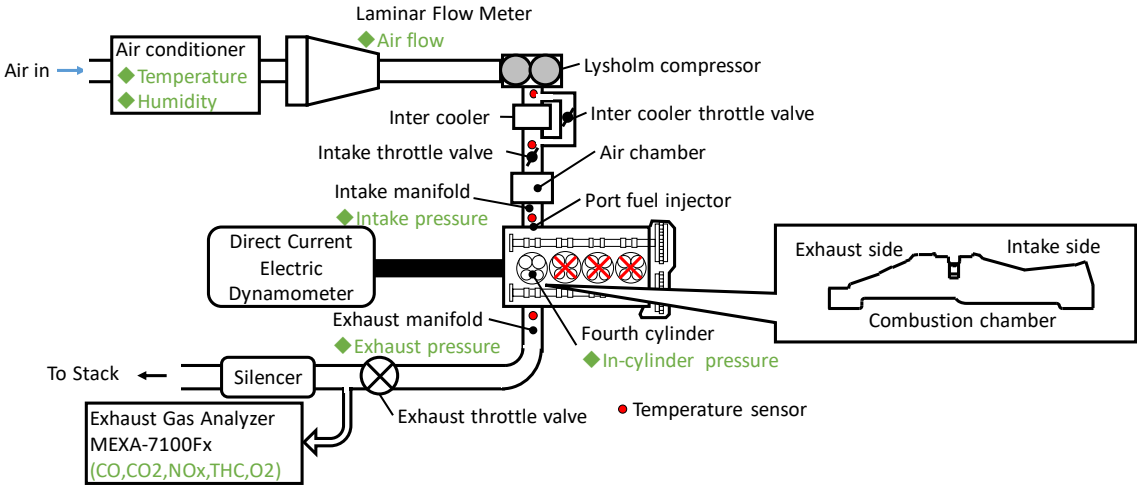

Figure 1: Schematic of the engine system for coil evaluation.

Table 1: Engine specification

Engine type	4 stroke engine
Bore x Stroke	79.7 mm x 81.3 mm
Displacement	404 cc
Compression ratio	12.2
Fuel supply system	Port fuel injection

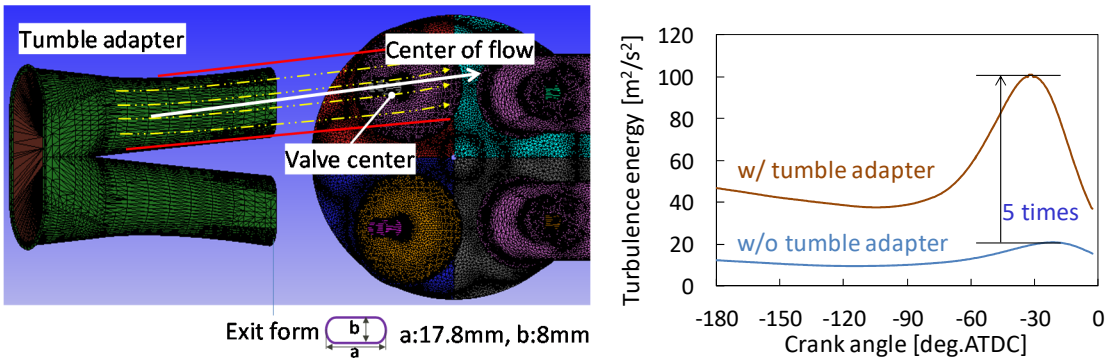

Figure 2: Schematic of tumble adapter (left) and estimation result of turbulent energy by using three-dimensional computational fluid dynamics simulation (right).

The engine equips optical window, and area around spark plug were taken by high speed camera (Photron: FASTCAM SA-X2) through an endoscope (KARLSTORZ:88370A).View angle of the endoscope is about 67degree and wide area from spark plug electrode to piston crown around top dead center can be observed. Fig. 3 is photo of in-cylinder and schematic of view area with description. Images were taken by a high speed camera with 40000 FPS (Frame Per Second) shutter speed and 23.4 μs exposure time. In this study, outer electrode of spark plug is located on center plane between intake valve and exhaust valve to prevent from disturbing tumble flow.

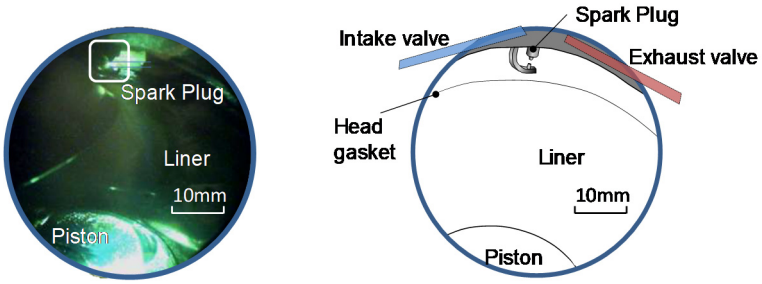

Figure 3: In-cylinder optical measurement area taken with high-speed camera through endoscope.

In order to measure discharge characteristics, both voltage of secondary coil (secondary voltage) and its current (secondary current) were measured. Fig.4 shows schematic of secondary voltage and current measurement system. Secondary current was measured by AC current prove (Person; Model 110A, reaction time 20ns), and secondary voltage was measured by high voltage prove (Tektronix; P6015A, reaction time up to 4.67ns). Sampling frequency of both current and voltage measurement are 1MHz. Output signal of both probes were measured by oscilloscope and data were transferred to PC through Ethernet. To reduce measurement noise, data were measured with Box Averaged model by the oscilloscope.

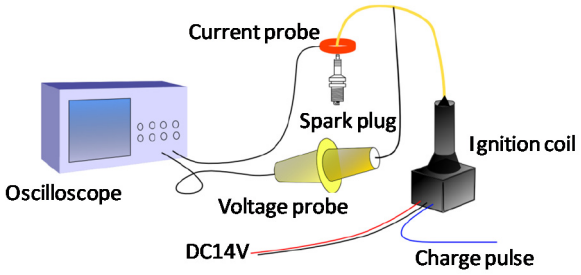

Figure 4: Secondary voltage and current measurement system.

In this study, five kinds of ignition coil were evaluated. As table 2 shows, though secondary energy of coil A, coil B and coil C is equivalent, maximum current of coil B and coil C are larger than coil A. Secondary energy of coil D is about twice of secondary energy of coil A. Coil E consists of two coil D which are parallel-connected and simultaneously discharged. Fig. 5 shows secondary current wave form of 5 coils. The secondary current waves on Fig. 5 were measured during engine test under 2000rpm engine speed and 0.6MPa NMEP. Maximum current value appears just after discharge start and current gradually reduces over time. Furthermore, secondary current oscillation due to restrike appears around end of discharge during engine test.

Table 2: Coil specification

No.	A	B	C	D	E
Secondary energy	86mJ	91mJ	97mJ	153mJ	274mJ
Peak secondary current	73mA	171mA	136mA	195mA	356mA
Spark duration	3.10ms	1.45ms	1.60ms	2.60ms	2.70ms

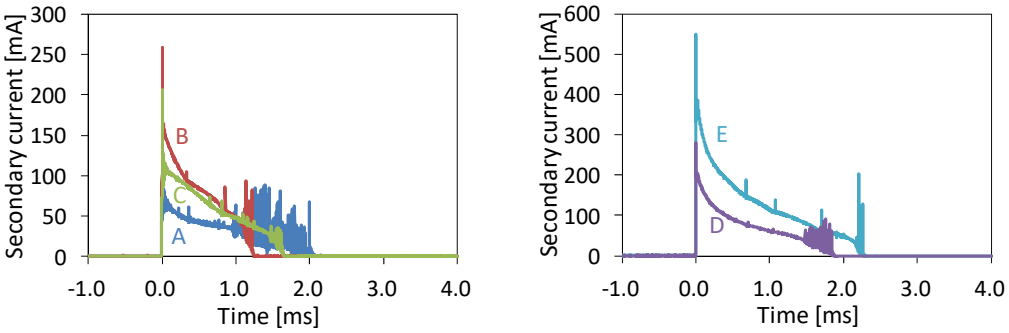

Figure 5: Secondary current form of each coil.

As coil evaluation test, two types of measurement test were conducted, one is combustion test which measures in-cylinder pressure, and another is optical measurement which conducts in-cylinder pressure measurement and optical access measurement simultaneously. Table 3 shows test conditions of combustion test and optical measurement. Engine speed is 2000rpm and fuel flow rate which achieves 0.6 MPa NMEP under stoichiometric combustion condition were applied to all test condition. Under combustion test, maximum air-fuel ratio realising stable engine combustion as dilution limit were investigated by increasing air-fuel ratio.

Table 3: Experimental conditions for combustion test and optical measurement

Control parameter	Combustion test	Optical measurement
Engine speed	2000 rpm	←
NMEP under stoic. condition	0.6 MPa	←
Coolant temperature	85 deg.C	←
Oil temperature	85 deg.C	←
Intake gas temperature	30 deg.C	←
Air Fuel ratio	14.7 ~ lean limit	23

Optical measurement were conducted under air-fuel ratio 23. In optical measurement, image recording by high-speed camera, measurement of secondary current, secondary voltage and in-cylinder pressure were conducted synchronously. Regarding in-cylinder optical measurement, discharge channel located between center electrode and grand electrode were recorded by taking visible light. According to recorded images, data relating with discharge channel behavior were measured. Fig. 6 shows discharge channel by visible light image taken by the camera. High voltage generated by ignition coil caused breakdown, and then discharge channel at spark plug gap emits visible light as shown on Fig. 6. Discharge channel was deformed by convection. In

this engine, flow direction at spark timing is from intake valve to exhaust valve, therefore the discharge channel stretchs to right hand side. Though flow direction around spark plug is not only horizontal direction of visualized plane but also vertical direction of the plane, the stretch of vertical direction were not acquired because the measurement was done from one observation point. Therefore, channel stretch to vertical direction of the plane was ignored. In this study, channel stretch is defined as distance from the line connecting electrodes to edge of the channel. Furthermore, channel stretch rate was calculated by ratio of channel stretch until 1st restrike and period from discharge start to 1st restrike occurrence.

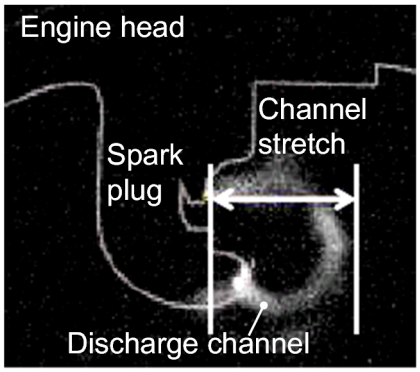

Figure 6: Definition of channel stretch.

3 Discussion

3.1 Dilution limit based on combustion test

In this section, air-fuel ratio limit of each coil, combustion index correlating with air-fuel ratio limit and relation between the index and coil specifications were investigated. Fig.7 shows air-fuel limit of each coil. Air-fuel ratio limit was defined as air-fuel ratio at coefficient of variation of NMEP by 3%. Fig.7 shows that the maximum air-fuel ratio limit of coil E is 24.6 and that of coil A is 23.1. Fig.8 shows relation between air-fuel limit and initial combustion period. Initial combustion period was defined as the period from spark timing until 10% of heat release was done. The initial combustion period of each coil were measured under air-fuel ratio 23 and spark timing 30 deg.BTDC. On fig.8, the dot shows average value of each coil and error bar shows standard deviation. As shown on fig. 8, it was confirmed that coil achieving shorter initial combustion period tends to lead larger air-fuel ratio. According to this result, initial combustion period under same conditions was clarified as a combustion index correlating with air-fuel ratio limit.

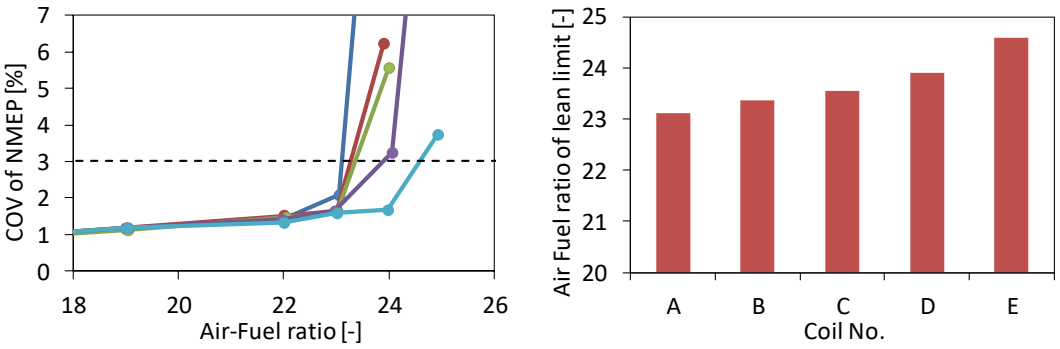

Figure 7: Coefficient of variance of NMEP over air-fuel ratio of lean limit (left) and air-fuel ratio of lean limit of each coil (right).

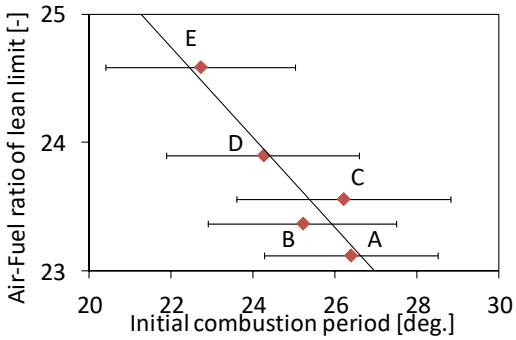

Figure 8: Air-fuel ratio of lean limit over initial combustion period. Diamond shows average value of each coil and error bar shows standard deviation.

As next step, coil specification to realize shorter initial combustion period was investigated. As a coil specification, secondary energy, average secondary power and average secondary current were selected.

$$E_S = \int_0^{t_D} I_S V_S dt$$

$$P_{ave} = \frac{1}{t_D} \int_0^{t_D} I_S V_S dt$$

$$I_{ave} = \frac{1}{10^{-3}} \int_0^{10^{-3}} I_S dt$$

Here, P_{ave} is average secondary power [W], t_D is discharge period [s], I_s is secondary current [A], V_s is secondary voltage [V], E_s is secondary energy, I_{ave} is average secondary current [A]. Average secondary power is average power from spark timing to end of discharge. Average secondary current is average secondary current during 1ms from spark timing. Secondary power and secondary current were selected as index relating coil generating power. Fig. 9 shows initial combustion period over secondary energy, Fig. 10 shows initial combustion period over average secondary current. All values on these figures are average value of 20 combustion cycles and error bar shows

standard deviation. Furthermore, linear interpolate line and determination coefficient were shown on figures. According to figure, larger secondary energy, average secondary power and average secondary current leads shorter initial combustion period. Among these three paramters, average secondary current shows the strongest correlation with initial combustion period.

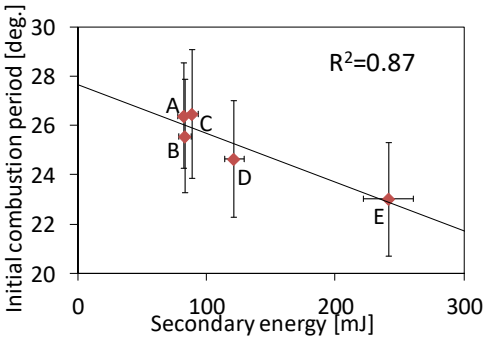

Figure 9: Initial combustion period over secondary energy.

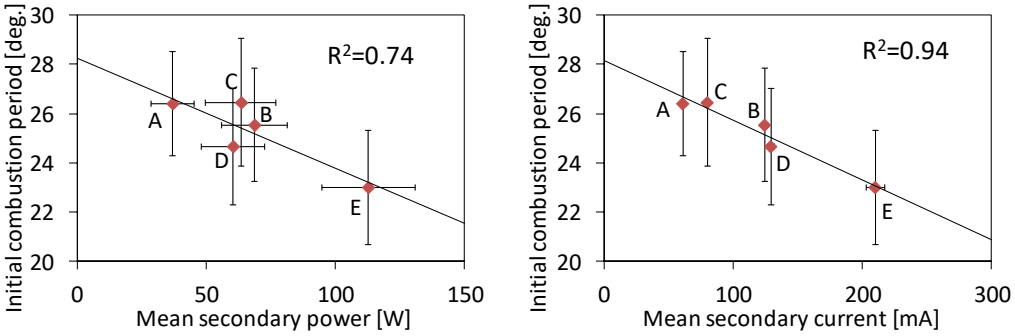

Figure 10/11: Initial combustion period over power related parameters, mean secondary power (left) and mean secondary current (right).

3.2 Analysis of combustion control factor based on optical measurement

Other index correlating with initial combustion period limit was investigated by analyzing discharge channel behavior taken by high-speed camera. In optical measurement, in-cylinder pressure at spark timing was 8.6 bar. According to a literature [1], discharge channel stretch rate might be close to flow velocity, therefore zero relative velocity between flow velocity and channel stretch rate was assumed in this study. With this assumption, mixture in discharge channel is assumed to be continuously heated from break down to restrike occurrence.

Since energy supply with mixture from discharge, mixture ignition, flame kernel formation and burning of a part of mixture by turbulent flame propagation might occur during initial combustion period, not only energy supply amount from discharge but also other physical parameters, such as flow velocity around spark plug, turbulence, mixture distribution and temperature distribution, might effect on initial combustion period [5]. Therefore, secondary energy from break down to 1st restrike occurrence and discharge channel stretch rate as index of flow velocity are selected as initial combustion period related parameters, and relation between initial combustion peri-od and these parameters were investigated.

Fig. 12 shows initial combustion period over channel stretch until 1st restrike. The left figure of fig. 12 shows average data classified by channel stretch and the right figure of fig.12 shows each cycle data. Though initial combustion period tend to decrease by increase of channel stretch until 1st restrike on Fig. 12, causal association among these are not clear and further investigation is required. .It was confirmed that variation of initial combustion period under same channel stretch condition is 8deg. Channel stretch is one of initial combustion period related index.

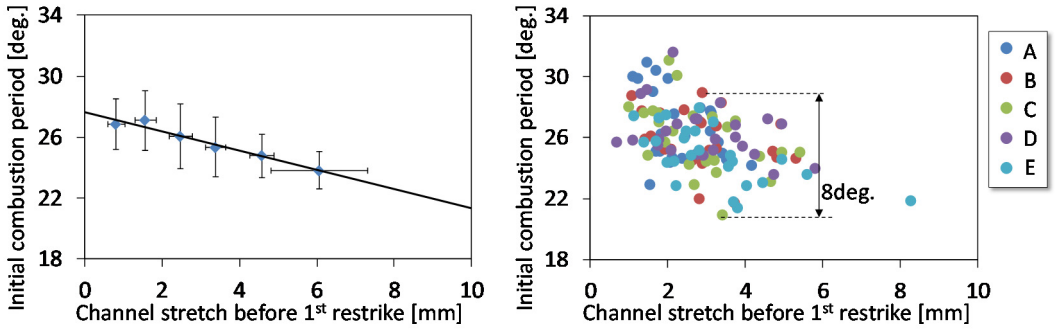

Figure 12: Initial combustion period over channel stretch until 1st restrike, mean value (left) and each cycle value (right).

Fig.13 shows initial combustion period over secondary energy until 1st restrike. The left figure of fig. 13 shows average data classified by channel stretch and the right figure of Fig.13 shows each cycle data. The left figure of Fig.13 shows initial combustion period tends to decrease by increase of secondary energy up to 50mJ. Furthermore, initial combustion period is saturated above 50 mJ. This result shows that increase of secondary energy until 1st restrike is effective to reduce initial combustion period reduction and upper limit of initial combustion period reduction by secondary energy increase exists. Since secondary energy until 1st restrike by coil E exceeds 50mJ every cycle, secondary energy and secondary current of coil E are sufficient enough, therefore initial combustion period is not reduced by further increase of secondary parameters. Fig.13 shows that variation of initial combustion period under same secondary energy until 1st restrike can be 8deg.

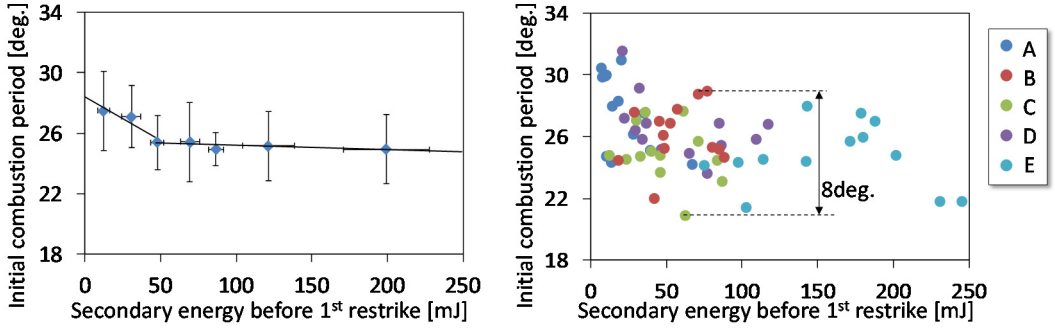

Figure 13: Initial combustion period over secondary energy until 1st restrike, mean value (left) and each cycle value (right).

Fig.14 shows initial combustion period over discharge channel stretch rate. The left figure of fig. 14 shows average data classified by channel stretch and the right figure of fig.14 shows each cycle data. The left figure on fig.14 shows initial combustion period tend to decrease by increase of channel stretch rate up to 20m/s. This result indicates larger flow velocity from intake valve side to exhaust valve side generates faster initial combustion period and consistent with investigation result by Furui et al [6]. Fig.14 shows that variation of initial combustion period under same channel stretch rate can be 9deg.

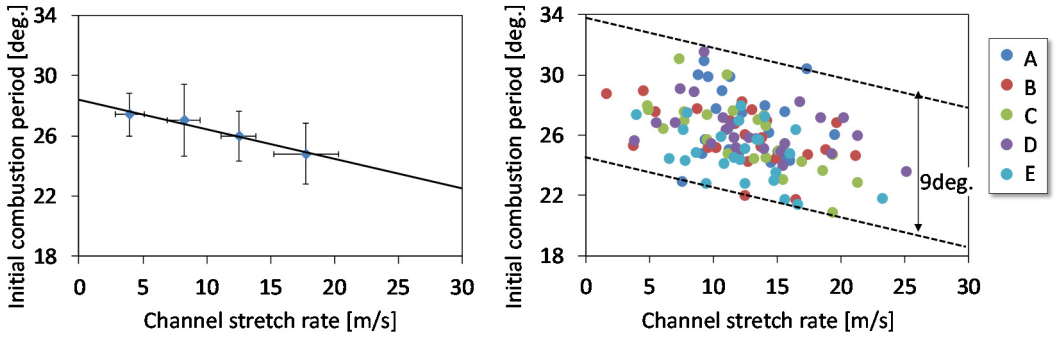

Figure 14: Initial combustion period over channel stretch rate, mean value (right) and each cycle value (left).

Further investigation was done by using Fig.15. Fig.15 shows initial combustion period distribution on a plane of channel stretch rate and secondary energy until 1st restrike. Fig.15 shows totally 18 data abstracted from measurement data of coil A, coil D and coil E. The three largest initial combustion period cycles and the three smallest initial combustion period cycles were selected. The circle size indicates initial combustion period. As discussed above, channel stretch rate affects initial combustion period, therefore data under a certain range of channel stretch rate was selected and was compared with each other.

Difference between maximum initial combustion period and minimum value of each coils are 6.8 by Coil A, 6.4 by Coil D and 6.5 by Coil E. Difference of these three coils are equivalent and it means that increase of secondary energy or secondary current does not affect to reduce variance of initial combustion period are not affected by under relatively stable control condition which coefficient of variation of NMEP is less than 3%.

Moreover, Fig.16 shows initial combustion period over channel stretch rate and initial combustion period over secondary energy until first restrike. The left figure on fig.16 shows data under secondary energy 10mJ, 21mJ and 64mJ. The right figure on fig.16 shows data under channel stretch rate 8.9m/s and 15.5m/s. Horizontal axis value are normalized by 66mJ for left figure and 18m/s for right figure. Initial combustion period change over channel stretch rate is steeper than that over secondary energy until first restrike. According to this result, flow around spark plug affects more on initial combustion period variation under this evaluation condition.

According to discussion of test under small variation of NMEP, increase of secondary energy or secondary current affects reduction of initial combustion period. Variation of initial combustion period, however, is not suppressed by increase of secondary energy

or secondary current. Moreover variation of the initial combustion period depends on in-cylinder flow condition.

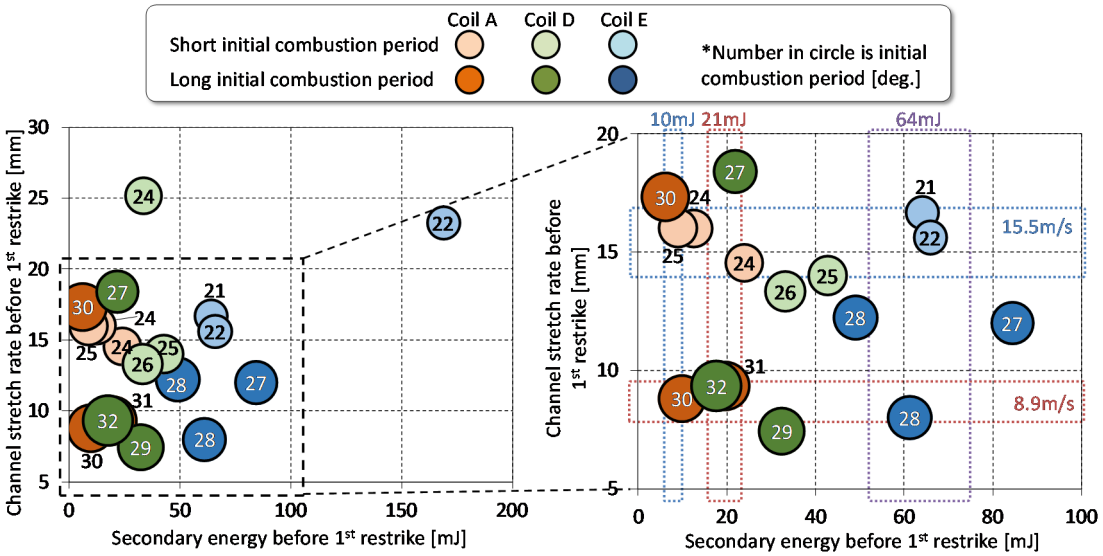

Figure 15: Initial combustion period on a plane of channel stretch rate and secondary energy until 1st restrike.

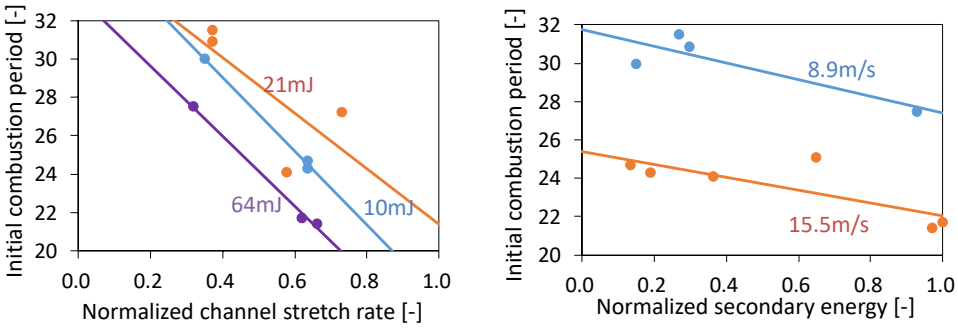

Figure 16: Initial combustion period over normalized channel stretch (left) and initial combustion period over normalized secondary energy until 1st restrike (right).

3.3 Vehicle test of selected coil

As discussed in section 3.2, channel stretch until 1st restrike is one of parameters correlating with initial combustion period correlating. Adequate coil specification for dilute combustion system was selected based on channel stretch. Fig.17 shows relation between channel stretch and secondary energy listed on table 2. As shown on Fig.17, channel stretch until 1st restrike seems to be saturated above 100mJ secondary energy. Then finally ignition coil generating 120mJ was selected including margin, and evaluated dilution combustion performance with vehicle which is 1.6liter turbo-charged direct injection engine.

EGR rate were calibrated for vehicle for demonstration. Fig. 18 shows EGR map above middle load conditions. The maximum EGR rate is more than 20% by mounting selected ignition coil. Finally, we drove the car on WLTC driving cycle and confirm fuel

consumption benefit. Fig. 19 shows history of fuel consumption and EGR rate over time. The test clarified that fuel consumption was reduced by 2.3% than original setting.

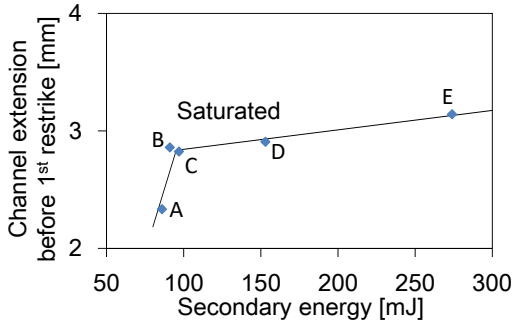

Figure 17: Channel stretch until 1st restrike over secondary energy

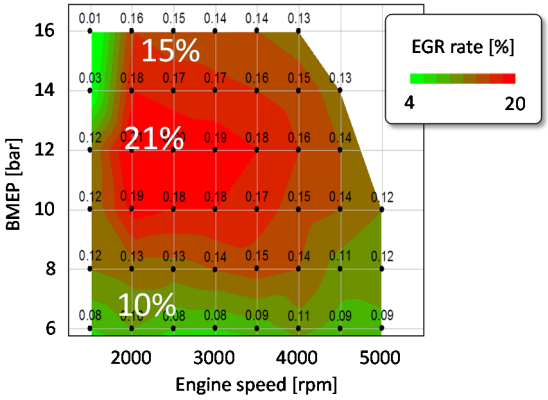

Figure 18: EGR rate map

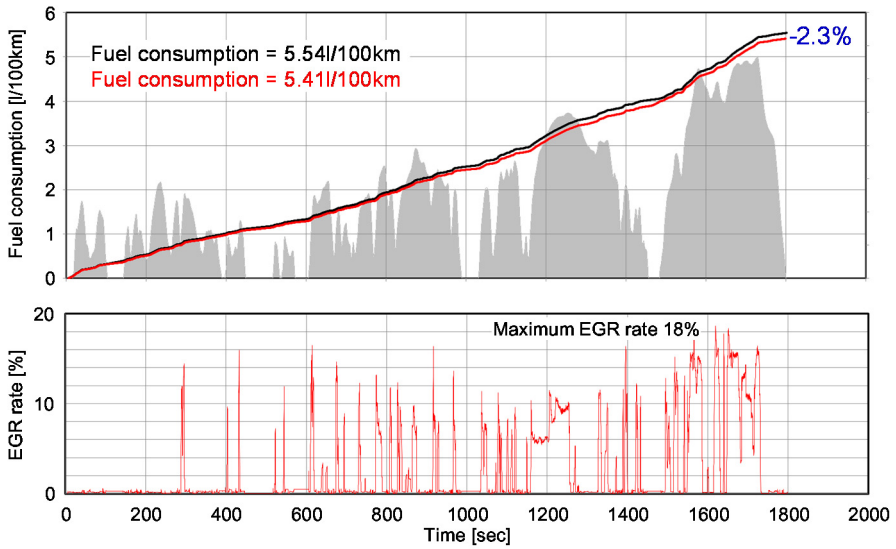

Figure 19: Fuel consumption and EGR rate profile on WLTC

4 Conclusion

In order to clarify effects of ignition specifications on combustion status and factors affecting on dilution limit, five coils generating different current profile were evaluated with combustion test and optical measurement by using a single cylinder engine. Finally, one opacification was selected based on channel stretch result and evaluated it on demonstration vehicle. Based on these investigation, followings were obtained.

- Initial combustion period measured under equivalent condition has correlation with dilution limit. It means that coils achieving shorter initial combustion period can extend dilution limit.
- Initial combustion period has correlation with coil secondary energy, average secondary power and average secondary current until 1ms. The average secondary current showed the largest correlation with initial combustion, average current until 1ms is adequate value for coil evaluation.
- Optical measurement test results showed a correlation of initial combustion period with discharge channel stretch.
- Under small variation of NMEP, increase of secondary energy or secondary current affects reduction of initial combustion period. Variation of initial combustion period, however, is not suppressed by increase of secondary energy or secondary current. Moreover variation of the initial combustion period depends on in-cylinder flow condition.
- Ignition coil generating 120mJ was selected and equipped on a test vehicle. The vehicle achieved maximum EGR rate more than 20% and 2.3% of fuel consumption reduction was confirmed by WLTC driving cycle test.

Literature

[1] Shiraishi, T., Teraji, A. and Moriyoshi, Y., The effects of ignition environment and discharge waveform characteristics on spark channel formation and relationship between the discharge parameters and the EGR combustion limit, JSAE 20159179, SAE 2015-01-1895 (2015).

[2] Brandt, M., Hettinger, A., Schneider, A., Senftleben, H. and Skowronek, T., Extension of operating window for modern combustion systems by high performance ignition, Ignition Systems for Gasoline Engines 3rd International Conference (2016), pp.26-51.

[3] Suzuki., K., Uehara, E. and Nogawa, S., Study of ignitability in strong flow field, Ignition Systems for Gasoline Engines 3rd International Conference (2016), pp.69-84.

[4] William, M. S., The algorithmic structure of the air/fuel ratio calculation, Readout HORIBA Technical Reports, No.15 (1997), pp.17-24.

[5] Johansson, B., Cycle to cylce variation in S.I engines – the effects of fluid flow and gas composition in the vicinity of the spark plug on early combustion, SAE Technical Paper 962084 (1996).

[6] Furui, T., Nishiyama, A., Minh, K., L., and Ikeda, Y., Analysis of in-cylinder flow and flame propagation in a gasoline engine using PIV, proceeding of JSAE meeting (spring) (2017), pp.1021-1026 (in Japanese).